Pathol. Oncol. Res. (2009) 15:315–322
DOI 10.1007/s12253-008-9111-3

ORIGINAL PAPER

Technical Feasibility of Transperineal MR-Guided Prostate Interventions in a Low-Field Open MRI Unit: Canine Study

Ferenc Lakosi · Gergely Antal · Csaba Vandulek · Arpad Kovacs · Rita Garamvolgyi · Ors Petnehazy · Gabor Bajzik · Janaki Hadjiev · Imre Repa · Peter Bogner

Received: 31 March 2008 / Accepted: 7 October 2008 / Published online: 23 October 2008

Abstract Magnetic resonance imaging (MRI) provides superior visualization of the prostate, its substructure, surrounding tissues, and, most important, focal lesions or cancer. The purpose of our canine study was to demonstrate the feasibility of a low-field (0.35 T) transperineal system that enables precise MR image guidance of prostate interventions. The canines were placed in the right lateral decubitus position. Template reconstruction, trajectory planning, contouring were based on T2-weighted FSE images. For image guidance and target confirmation, fast gradient spoiled-echo (FSPGR) sequence was used. MR compatible coaxial needles were manually inserted through the perineum to the base of the prostate. After satisfactory position was confirmed, brachytherapy catheters were placed through the coaxial needles. The mean deviation of the needle displacements was 2.9 mm with a median value of 2.7 mm. 97% of the errors were less than 4.0 mm. The needle placement accuracy was modelled by the Rayleigh distribution with a sigma value of 2.3 mm. Visual confirmation of needle placements was demonstrated on pathology tissue slices. The time needed for each step was: anaesthesia - 15 min, setup and positioning - 15 min, initial imaging - 15 min, template registration, projection - 15 min, contouring, trajectory planning, insertion of 12 needles - 60 min Based on our canine experiences our method seems to be a promising approach for performing feasible, accurate, reliable and high-quality prostate MR guidance within a reasonable time span.

F. Lakosi · G. Antal · C. Vandulek · A. Kovacs · R. Garamvolgyi · O. Petnehazy · G. Bajzik · J. Hadjiev · I. Repa · P. Bogner (✉)
Health Science Center, University of Kaposvar,
Guba Sandor Street 40,
Kaposvar H-7400, Hungary
e-mail: bogner.peter@sic.hu

Keywords Prostate cancer · Interventional · Brachytherapy · MR-guidance

Introduction

Prostate cancer is the most common male malignant disease in the Western world. In Hungary, 2,839 new cases were registered in 2001, while in 2004 more than 4,000 new cases of prostate cancer were diagnosed. However, the mortality rate has not changed [1].

Data from the phase III prospective randomized trials showed that biochemical control rates could be improved if the delivered dose to the prostate gland is increased [2]. Besides the modern external-beam techniques including three dimensional conformal radiotherapy (3D-CRT) or intensity-modulated radiotherapy (IMRT), brachytherapy could be a feasible method for local dose escalation [3]. The essence of interstitial brachytherapy is to place radioactive sources directly into the prostate gland by using transperineally inserted needles. Based on the inverse square law, either form of brachytherapy could achieve a high radiation dose in the close vicinity of the sources that being the implanted prostate, with a rapid dose decline beyond the gland preserving surrounding normal tissues. This form of dose level control is more difficult to be reached by the external beam techniques.

The gold standard technique for guidance of prostate biopsy and brachytherapy is transrectal ultrasound (TRUS) due to the ease of use, low costs and fast, real-time image acquisition [4]. However, magnetic resonance imaging (MRI) seems to have several advantages over US. For instance, excellent soft tissue contrast, high sensitivity for detecting prostate tumors, high spatial resolution and multiplanar volumetric 3D imaging capabilities [5]. Func-

tional MRI imaging methods like spectroscopy, dynamic contrast studies, and diffusion weighted images not only provide essential structural description, but also additional molecular and metabolic information. [6]–[10] Thus, beside the biologic knowledge of the disease by the visualization of the intraprostatic dominant lesion targeted interventions, partial radiation dose delivery, and dose painting became possible.[9], [10] These characteristics led to the integration of MRI into the image-guided procedures. The utility and clinical efficacy of MR-guided prostate brachytherapy and biopsy has been demonstrated by an increasing number of groups.[11]–[20]

These experiences facilitate us to introduce MR-guided prostate brachytherapy and biopsy in our institution also. In the first step we initiated a canine study to develop and perfect our technique in an open 0.35 T MRI scanner. We report our results with respect to the methodology, needle placement accuracy, image quality, intervention tolerance and working time analysis. Having demonstrated the feasibility and consistency in our technique, the trial will now proceed to a pilot clinical trial.

Materials and Methods

Positioning, Device Description

Prostate interventions were performed on 6, old mongrel dogs in an open-configuration 0.35 T MRI scanner (Signa Ovation; General Electric Healthcare; Milwaukee; USA). The study protocol was approved by the regional ethical committee of animal care (record number: 246/002/SOM/2006). Because of the design of the scanner, the interventions were performed with the canine placed in the right lateral decubitus position (Fig. 1). For interventions, an MR compatible device was developed consisting of three major parts: template-obturator rod, immobilization arm and transport tray. The obturator was a 1.8–2.4 cm diameter rod, which was inserted into the rectum. The template was affixed perpendicular to the obturator and placed against the perineum. The exact position of the template was difficult to be controlled because of the gluteal tissues, thus an assisted template parallel with the first was affixed to the obturator. On this second template guiding lines were grooved in the horizontal and coronal planes and were used for the correct alignment of the built-in laser lines of the MR scanner. The cylindrical end of the obturator was perpendicularly fitted to the immobilization stage. In addition to the holding mechanism, the positioning stage contains a screw-drive mechanism that allows rotation, translation, or vertical movement of the template-obturator rod. The patient tray fitted soundly on the table and allowed for device and patient immobilization (Fig. 1).

Fig. 1 Canine and device positioning in the open magnet. Note the patient tray and the right lateral decubitus position. Needle insertions are performed from the posterior profile of the MR scanner

Imaging

The pelvis was imaged using the manufacturer's 9-inch GP (general purpose) surface coil. After the positioning of the device the coil was placed around the template-obturator rod and pressed against the gluteal masses.

Two different pulse sequences were used for imaging. A T2-weighted fast spin-echo (FSE) (repetition time (TR) 3,100 ms, echo-time (TE) 86 ms, Flip Angle (FA) 56°, pixel bandwidth (BW) 13.89 Hz, field of view (FOV) 32 cm, slice thickness/spacing 5/0 mm, 256×192, 30 slices, Number of Excitations (NEX) 4, scan time 7:36 min) and a T1-weighted fast spoiled gradient echo (FSPGR) (TR 100 ms, TE min, FA 60°, BW 10.42 Hz, FOV 32 cm, slice thickness/spacing 5/0 mm, 256×192, six slices, NEX 6, scan time:60 s) sequences were used in the axial, coronal and sagittal plane. On the axial T2 FSE sequences the image volume extended from the template to the prostate base plane. These images were used for the template reconstruction, trajectory planning and contouring. The FSPGR sequence was used for image guidance and the quick verification of the position of the MR compatible coaxial needles. The imaging time was approximately 8-10 s/image. The imaging volume covered the whole prostate.

Template Reconstruction, Trajectory Planning

The rationale of reconstruction was that the template with the obturator composed a fix geometric unit being perpendicular to each other. Thus ideally the needle direction through the template was parallel to the longitudinal axis of the obturator. The first step of template

reconstruction was the filling of the template holes with sterile surgical gel (Instillagel; Farco-Pharma Gmbh; Cologne; Germany) which allowed for a clear visualization of the template grid on T2 FSE images (Fig. 2). Then using our treatment planning system (Theraplan Plus version 3.8; Anatomy Modelling; MDS Nordion; Quebec; Canada)—running on a PC networked to the MR scanner—the template grid was defined with a standard triangle grid-geometry punch pattern with a polygon-contour (easily manageable by the designer system). Its apices represented the template-holes and closed through a standard hexagon outlining the obturator, thus making up a unified, so-called template-obturator contour (TOC) (Fig. 2). This contour, by means of an adequate shifting and rotation, could be adjusted onto the axial MR-image of the template. After the grid was fully registered, the virtual template-obturator contour was projected on the consecutive axial slices from the template to the bladder neck (Fig. 2). The target depth for all needles was the prostate base plane. Its distance from the template was represented on the axial MR images.

Catheter Placement

Before interventions the canines underwent bowel preparatory regimen and antibiotic prophylaxis (Shotapen 250 ml injection IM (Virbac); benzylpenicillin 10 g, dihydrostreptomycin 16.4 g/100 ml; dosage: 1 ml/20 kg). All procedures were performed under endo-tracheal general anesthesia. A urinary catheter was inserted into the bladder and clamped. After a digital rectal examination, preparation, sterilization and isolation of the perineum, the canines were placed feet first in the right lateral decubitus position on the tray. The obturator was gently inserted into the rectum and at the same time the jelly filled template was placed firmly against the perineum. The template-obturator rod was then attached to the immobilization arm which is already fixed on the patient tray. The coil was positioned, as described previously, and secured to the table and the gluteal masses of the canine. Imaging started with a 3D localizer followed by the T2 FSE and T1 FSPGR sequences in all three planes. The axial slices were then digitally forwarded to the planning system. The prostate, rectum, urethra, bulbus and the pubic arch were delineated (Fig. 2). Template reconstruction and trajectory planning followed. The potential puncture points were recorded on a printed format of the template, which was posted on the navigation table as well as the scanning room. For the visual feedback MR images are continuously projected onto screen within the MRI scanner room. For catheter placement MRI compatible coaxial needles (14G; In vivo Germany GmbH; Schwerin; Germany) were used. The locations of the needles were confirmed by using the above mentioned FSPGR sequences. The location of the needle tip artifact relative to the selected grid point was compared by two authors (F.L., G.B.)

After satisfactory position of the needle was confirmed (Fig. 2), the inner mandrin was removed and a plastic brachytherapy catheter (5F; Proguide; 240 mm; Nucletron; Veenendaal; The Netherlands) was inserted through the

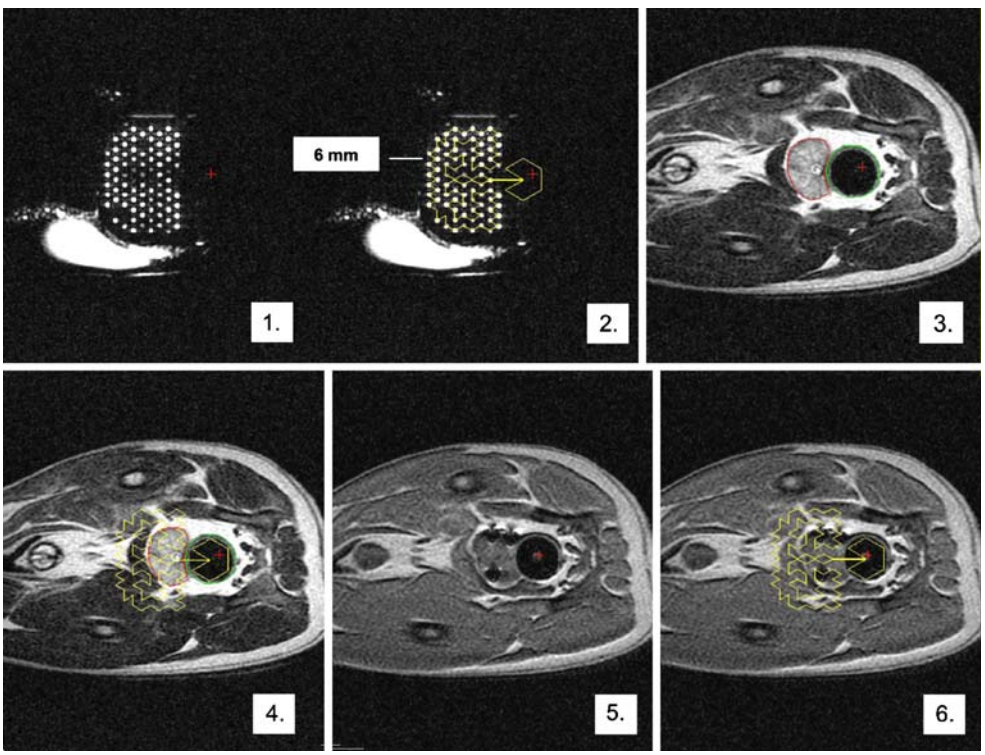

Fig. 2 Template holes filled with jelly are easily recognized on T2-weighted images. **(1)** Fitted template-obturator contour (TOC) (*yellow*). **(2)** Contouring (*prostate: red, urethra: light blue, rectum: green*). **(3)** Projected TOC on the consecutive axial slices. **(4)** Inserted coaxial needles within the prostate on FSPGR sequences. **(5)** Target confirmation by the superimposed template holes. It shows less than 3 mm target accuracy for all of the inserted needles. **(6)**

coaxial needle. The outer part of the coaxial needle was then removed. After all plastic catheters were inserted, a set of T2-weighted FSE images with 3 mm slice thickness were acquired to help verify whether each catheter reached the prostate base plane. If necessary a final reposition could be made.

For studying the visual control of needle placement accuracy, in one canine the catheters were inked with alcyan-blue and then inserted through the coaxial needles. At the end of the implantation there was no willingness to perform control T2-weighted FSE images. Immediately following the implantation and the sacrificing of the animals, the canine prostate was removed and fixed in formalin. After 24 hours it was sliced into 3 mm sections, photographed and paired with the corresponding MR image sections by two authors (F.L., G.B.)

Results

Intervention Tolerance

In general, the interventions were well tolerated. There were no serious intervention related adverse events (i.e. injury of the urethra, rectal and bladder wall, extensive bleeding), neither in the intra-operative nor in the post-operative period. All of the canines except the sacrificed one recovered within 2 days.

Image Quality

Despite the fact that a 9-inch GP coil was used for pelvic imaging, our sequences allowed clear definition of the prostate, urethra, periprostatic tissues as well as the coaxial needles and brachytherapy catheters in all cases (Fig. 3a–d).

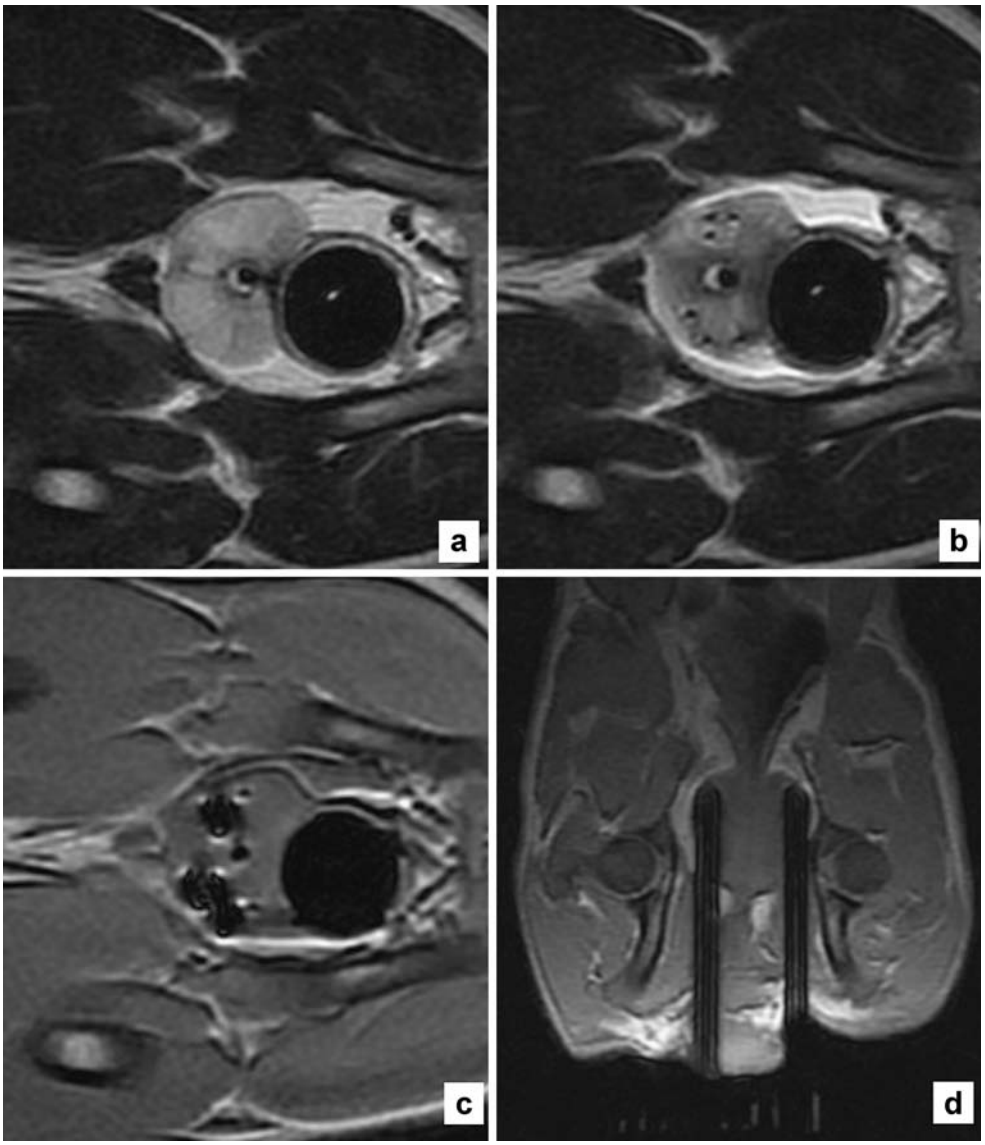

Fig. 3 T2-weighted axial FSE images before **(a)** and after implantation **(b)**. Besides the prostate and the urethra plastic catheters are easily and clearly visualized as small black dots. Axial **(c)** and coronal **(d)** view of T1-weighted FSPGR images with the inserted coaxial needles. Simultaneously plastic catheters are well depicted

To interpret the results of the needle placement study mentioned below, it is necessary to examine the artifact effect of the 14-G coaxial needle. On T1-weighted FSPGR sequences the coaxial needle artifacts were easily recognized due to the susceptibility-effect. Due to the design of the needle placement system, the needles are approximately 90° to the static magnetic field. In this situation—confirmed by our preliminary gel studies—the needle artifacts were presented as 10 mm in width circular, black voids and the tips of the needle artifacts were depicted 3–4 mm deeper within the tissue then the actual position of the needle (Fig. 3c,d). Therefore the artifact position is a good estimate of the needle tip position. Plastic catheters were also well depicted on the gradient-echo images; however, the clear definition was limited in the close vicinity of the coaxial needles due to artifact effect and the relatively low signal to noise ratio (SNR).

T2-weighted FSE images had their advantages in demonstrating prostate parenchyma, urethra, prostate-rectum interface and the plastic catheters. All plastic catheters were clearly visualized on these sequences (Fig. 3a,b).

Needle Placement Accuracy

The target depth was determined as the level of the prostate base. The mean displacement of the coaxial needles at this target depth was calculated using the following method. We have separately recorded the **x** and **y** coordinates of the center of the coaxial needle artifact and the intended target site (i.e. the projection of the virtual template hole) and then determined the difference between them. The overall deviation was calculated using the following formula:

$$R = \sqrt{x^2 + y^2}$$

Altogether, 37 coaxial metal needles and plastic catheters were inserted with an average target depth of 11 cm (range: 10.5–12.5 cm). Mean deviation of the needle displacements was 2.9 mm, with a median of 2.7 mm. 97% of the errors were less than 4.0 mm; maximum error measured was 4.5 mm. The needle placement accuracy was modeled by the Rayleigh distribution with a sigma value of 2.3 mm (Fig. 4).

Pathology Study

In one canine, visual confirmation of eight needle placements was demonstrated. Fig. 5 shows that despite the prostate deformation caused by the obturator, the distribution of the stained catheter trajectories seen in the specimen slices clearly and favorably matches with the distribution of the plastic catheters as visualized on transverse T1-weighted FSPGR sequences. The catheters were numbered consecutively from the left to the right side of the prostate.

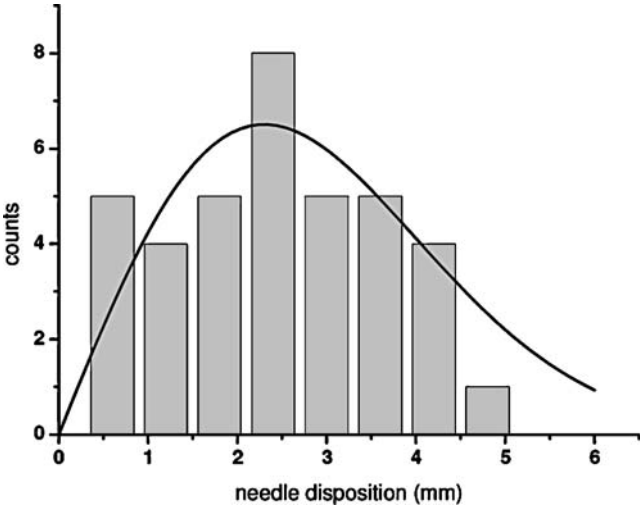

Fig. 4 Needle placement accuracy diagram for the 37 coaxial needle insertions with the maximum-likelihood Rayleigh distribution

On the basis of the MR findings there was a good agreement between the authors (F.L., G.B.) in considering that catheter 1 had not entered into the periphery of the left lobe of the prostate and three catheters (number 2,6,8) had not reached the base plane. This was also confirmed by the pathology tissue slices respectively (Fig. 5).

Working Time Analysis

The overall time of the interventions in the MR unit, determined from the induction of anesthesia to extubation, gradually improved procedure by procedure. The total time of the final procedure, in which 12 catheters were implanted, was 2 hours. The time needed for each step were the following: anesthesia - 15 min, setup and positioning - 15 min, initial imaging - 15 min, template registration and projection - 15 min, contouring, trajectory planning, needle insertion - 60 min.

Discussion

The excellent soft tissue contrast achieved by MRI was the rationale for the introduction of MRI data in the cross sectional imaging guided and assisted interventions. In gynecological tumors, MR-assisted brachytherapy treatments are becoming more and more popular [21]. However, only a limited number of publications are available considering MR-guided prostate interventions especially brachytherapy [12–15, 17, 18]. MR-guided prostate interventions could be classified into three groups based on methodology.

The first, most common approach is to fuse the diagnostic MR image information with the “gold standard” ultrasound images [9]. Its major advantage is the US guidance due to

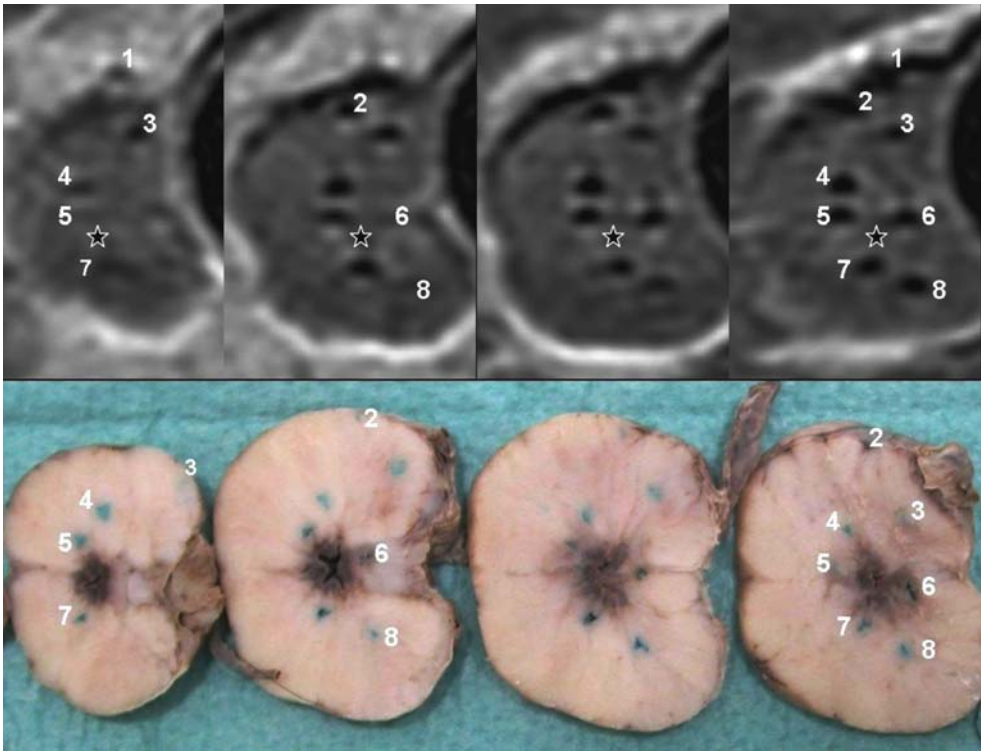

Fig. 5 Corresponding MR *(top)* and specimen slices *(bottom)* from the base plane of a canine prostate (*left to right*). Good agreement could be visualized in the distribution of the stained needle tracts and the plastic catheters *(white numbers)*. Urethra *(black star)* was carefully avoided by the catheters

its fast image acquisition, ease of usage, low cost, wide availability in most centers and less technical background.

The second method is the use of open configuration MRI scanners both for image guidance and for treatment planning. These systems offer improved and convenient access to the patient during the procedure. Its major drawback compared to high-field MR systems, is the reduction of signal to noise ratio leading to a decrease in image quality. The clinical efficacy of MR-guided transperineal permanent seed implantation and biopsy was demonstrated by D'Amico, Tempany et al [12, 13] at the Brigham and Women's Hospital using a 0.5 T open MR unit. The interventional magnet was modified for side entry and lithotomic patient positioning allowing simultaneous catheter placement and imaging. Zangos et al [19] described the technical feasibility of transgluteal biopsy on 0.2 T open MR. However, both approaches mentioned above simplify the interventional procedure itself; there is a need for deformable image registration in order to integrate the diagnostic and functional information.

The third approach involves performing interventions in high-field closed bore 1.5–3 T MR systems [11, 15–18, 20]. The major advantage of this method is the excellent image quality as well as the ability to directly incorporate molecular and metabolic knowledge of the most likely locations of tumors within the gland. Menard, Susil et al [17, 18] were the first who performed transperineal biopsy and HDR brachytherapy on a 1.5 T MR unit. The patient was positioned in the left lateral decubitus position and withdrawn from the magnet bore for needle insertions, then advanced back into the scanner for target confirmation. MR-guided transrectal targeted biopsies with high-field systems were performed in Europe also [11, 16]. The main limiting factors of using closed magnets for interventions are the patient dimensions and the difficult access to the perineal region without withdrawing the patient from the bore. For this reason and for the improved navigation, computer integrated robot assistant systems, short bore high field MRI scanners have been developed [13–15].

For MR-guidance, a low-field open MRI system is available at our Institution. In this canine study we have developed and presented the complex methodology of MR-guided prostate HDR brachytherapy, which could be entirely adapted to humans. Since the technique can be suitable for transperineal targeted biopsy, the custom made device was designed to be appropriate for interventions in our 1.5 T MR unit as well.

Several challenges had to be overcome before the implementation of this methodology. Reliable definition of the target area, urethra, intraprostatic catheters are important aspects that significantly influence the quality of brachytherapy. On the other hand, very fast image acquisition was also mandatory for MR guidance. Our goal was to use specially adapted pulse sequences on the 0.35 T MR scanner which could fulfill these criteria. The design of the scanner allowed for only lateral decubitus positioning of the patient. However, this type of patient positioning prevented the use of the manufactured pelvic or body coil.

Therefore, we used the 9-inch GP coil for the pelvis imaging. This imaging technique with the previously described pulse sequences allowed for excellent visualization of the prostate, organs at risks, coaxial needles and plastic catheters during the entire procedures. Furthermore, these sequences were also successfully tested on healthy volunteers and prostate cancer patients. Also important was the fact that the GP coil did not compromise neither the appropriate access to the template nor the needle insertions.

Similarly to Susil et al [18], we used surgical jelly for template registration. This method not only provided convenient and reliable registration, but connected with the rectal contour allowed fast and correct adjustments of the projected template grid through the whole trajectory on the FSPGR sequences.

Limited data are available concerning the accuracy of needle placement during MRI-guided prostate interventions. DiMaio et al [14] have measured the insertion errors during transperineal biopsy in four patients on a 0.5 T MR system at BWH. Using fast gradient recalled sequences, the average distance of the planned and actual position of the 18G needles was 6.93 mm with a standard deviation of 0.93 mm. Susil et al [18] have also evaluated the needle placement accuracy of 32 transperineal biopsies using a 1.5 T conventional MR system. Their results showed a mean needle displacement of 2.1 mm with a maximum error of 4.4 mm. We have also used stiffer 14G needles for the 37 procedures and the average needle accuracy experienced was 2.9 mm, 97% of the needle placement errors were less than 4 mm and the maximum error was 4.5 mm. It should be mentioned, that the target depth was more than 10 cm for all of the needles. The fine agreement in the distribution of the catheters visualized on MRI and pathology tissue slices also confirmed the reliability of our method. Similar to Susil et al [18], the distribution of the displacements even with a larger sigma value could be modeled by the Rayleigh distribution, which assumes that systematic errors do not exist in the different directions. Through our registration method, it appeared that these biases may be dominantly caused by the needle deflection in the soft tissues. Our development studies also confirmed these observations. Testing with a gel phantom and bovine kidney the observed tip error was consistently under 1 and 1.5 mm.

One of the disadvantages of MR-guided procedures is the prolonged working time. Menard et al [17] performed their first MR-guided HDR brachytherapy in 8.5 hours on a 1.5 T MR scanner. As they gained more experience, the overall procedure time was decreased less than 5 hours using an inverse planning system with larger number of coaxial needles between the verifications. Because of the importance of the time factor, special attention was given to the working time analysis. Our last intervention, during which 12 catheters were inserted, was performed in two hours. Although this time is acceptable, we believe that higher level of team experiences, strict working protocols and the use of more coaxial needles could result in additional improvements in the procedure time.

A system for transperineal MR-guided prostate intervention has been developed and applied successfully on canines. This method seems to be a promising approach for performing feasible, accurate, reliable and high-quality image guidance within a reasonable time span. Our results facilitate us to introduce MR-guided HDR brachytherapy as well as biopsy into the daily clinical practice in the near future.

References

1. Ottó S, Kásler M (2005) A hazai és nemzetközi daganatos halálozási és megbetegedési mutatók alakulása. Magyar Onkológia 49:99–107
2. Jereczek-Fossa BA, Orecchia R (2007) Evidence-based radiation oncology: definitive, adjuvant and salvage radiotherapy for non-metastatic prostate cancer. Radiother Oncol 84:197–215
3. Morton G (2005) The emerging role of high-dose-rate brachytherapy for prostate cancer. Clin Oncol 17:219–227
4. Presti JC Jr (2000) Prostate cancer: assessment of risk using digital rectal examination, tumor grade, prostate-specific antigen, and systematic biopsy. Radiol Clin North Am 38:49–58
5. Futterer J (2007) MR imaging in the local staging of prostate cancer. Eur J Radiol 63:328–334
6. Morgan VA, Kyriazi S, Ashley SE et al (2007) Evaluation of the potential of diffusion-weighted imaging in prostate cancer detection. Acta Radiol 48:695–703
7. Alonzi R, Padhani AR, Allen C (2007) Dynamic contrast enhanced MRI in prostate cancer. Eur J Radiol 63:335–350
8. Mueller-Lisse UG, Scherr MK (2007) Proton MR spectroscopy of the prostate. Eur J Radiol 63:351–360
9. Pouliot J, Kim Y, Lessard E et al (2004) Inverse planning for HDR prostate brachytherapy used to boost dominant intraprostatic lesions defined by magnetic resonance spectroscopy imaging. Int J Radiat Oncol Biol Phys 59:1196–1207
10. Van Lin EN, Futterer JJ, Heymink SW et al (2006) IMRT boost dose planning on dominant intraprostatic lesions: gold marker-based three-dimensional fusion of CT with dynamic contrast-enhanced and 1H-spectroscopic MRI. Int J Radiat Oncol Biol Phys 65:291–303
11. Beyersdorff D, Winkel A, Hamm B et al (2005) MR imaging-guided prostate biopsy with a closed MR unit at 1.5 T: initial results. Radiology 234:576–581
12. D'Amico AV, Cormack R, Tempany CM et al (1998) Real-time magnetic resonance image-guided interstitial brachytherapy in the treatment of select patients with clinically localized prostate cancer. Int J Radiat Oncol Biol Phys 42:507–515
13. Fischer GS, Di Maio SP, Haker SJ et al (2006) A system for MR-guided prostate interventions. Proceedings of 1st IEEE/RASD-EMBS International Conference on Biomedical Robotics and Biomechatronics February 2006, 68–73
14. Di Maio SP, Pieper S, Chinzei K (2007) Robot-assisted needle placement in open MRI: system architecture, integration and validation. Comput Aided Surg 12:15–24

15. Fischer GS, DiMaio SP, Iordachita II et al (2007) Robotic assistant for transperineal prostate interventions in 3 T closed MRI. Med Image Comput Comput Assist Interv Int Conf Med Image Comput Comput Assist Interv 10:425–433
16. Engelhard K, Hollenbach HP, Kiefer B et al (2006) Prostate biopsy in the supine position in a standard 1.5-T scanner under real time MR-imaging control using a MR-compatible endorectal biopsy device. Eur Radiol 16:1237–1243
17. Menard C, Susil RC, Choyke P et al (2004) MRI-guided HDR prostate brachytherapy in standard 1.5 T scanner. Int J Radiat Oncol Biol Phys 59:1414–1423
18. Susil RC, Camphausen K, Choyke P et al (2004) System for prostate brachytherapy and biopsy in a standard 1.5 T MRI scanner. Magn Reson Med 52:683–687
19. Zangos S, Eichler K, Engelmann K et al (2005) MR-guided transgluteal biopsies with an open low-field system in patients with clinically suspected prostate cancer: technique and preliminary results. Eur Radiol 15:174–182
20. Zangos S, Hercog C, Eichler K (2007) MR-compatible assistance system for punction in a high-field system: device and feasibility of transgluteal biopsies of the prostate gland. Eur Radiol 17:1118–1124
21. Potter R, Haie-Meder C, Van Limbergen E et al (2005) Recommendations from gynaecological (GYN) GEC ESTRO working group (II): concepts and terms in 3D image-based treatment planning in cervix cancer brachytherapy—3D dose volume parameters and aspects of 3D image-based anatomy, radiation physics, radiobiology. Radiother Oncol 78:67–77